Alzheimer's Disease Risk Gene, *GAB2*, is Associated with Regional Brain Volume Differences in 755 Young Healthy Twins

Derrek P. Hibar,[1] Neda Jahanshad,[1] Jason L. Stein,[1] Omid Kohannim,[1] Arthur W. Toga,[1]
Sarah E. Medland,[2,3,4] Narelle K. Hansell,[2] Katie L. McMahon,[5] Greig I. de Zubicaray,[6]
Grant W. Montgomery,[2] Nicholas G. Martin,[2] Margaret J. Wright,[2] and Paul M. Thompson[1]

[1]*Laboratory of Neuro Imaging, Department of Neurology, UCLA School of Medicine, Los Angeles, USA*
[2]*Genetic Epidemiology Laboratory, Queensland Institute of Medical Research, Brisbane, Australia*
[3]*Quantitative Genetics Laboratory, Queensland Institute of Medical Research, Brisbane, Australia*
[4]*Broad Institute of Harvard and MIT, Boston, USA*
[5]*Centre for Advanced Imaging, University of Queensland, Brisbane, Australia*
[6]*Functional Magnetic Resonance Imaging Laboratory, School of Psychology, University of Queensland, Brisbane, Australia*

The development of late-onset Alzheimer's disease (LOAD) is under strong genetic control and there is great interest in the genetic variants that confer increased risk. The Alzheimer's disease risk gene, *growth factor receptor bound protein 2-associated protein* (*GAB2*), has been shown to provide a 1.27–1.51 increased odds of developing LOAD for rs7101429 major allele carriers, in case-control analysis. *GAB2* is expressed across the brain throughout life, and its role in LOAD pathology is well understood. Recent studies have begun to examine the effect of genetic variation in the *GAB2* gene on differences in the brain. However, the effect of *GAB2* on the young adult brain has yet to be considered. Here we found a significant association between the *GAB2* gene and morphological brain differences in 755 young adult twins (469 females) ($M = 23.1$, $SD = 3.1$ years), using a gene-based test with principal components regression (PCReg). Detectable differences in brain morphology are therefore associated with variation in the *GAB2* gene, even in young adults, long before the typical age of onset of Alzheimer's disease.

∎ **Keywords:** *GAB2*, imaging genetics, tensor-based morphometry, Alzheimer's disease

Numerous heritability studies show that brain structure is under moderately strong genetic control (Kremen et al., 2010; Peper et al., 2007; Thompson et al., 2001). However, very few genetic variants have been identified that reliably explain a significant proportion of brain variation in human populations. Several researchers advocate the use of brain measures to empower the search for disease risk genes (Bis et al., 2012; Meyer-Lindenberg & Weinberger, 2006; Stein et al., 2012). If specific genetic variants can be related to brain differences, they may offer new molecular targets for drug development, and a deeper understanding of disease susceptibility and treatment response. For example, young adult carriers of a recently discovered risk allele for Alzheimer's disease (AD), *CLU*-C, have detectable differences in brain integrity approximately 50 years before the typical age of AD onset (Braskie et al., 2011), as do carriers of a common variant in an iron-overload gene, *HFE* (Jahanshad et al., 2012). Brain measures related to ge-

netic liability can be helpful for studying factors that may avert or promote disease (Gogtay et al., in press), and for defining the biological spectrum underlying psychiatric disorders (Akil et al., 2010). For instance, carriers of the common Val66Met polymorphism in the brain-derived neurotrophic factor (*BDNF*) gene are at heightened risk for bipolar disorder (Fernandes et al., 2011) and schizophrenia (Green et al., 2011). They show detectable differences in white matter microstructure (Chiang et al., 2010),

hippocampal volume (Hajek et al., 2012), and prefrontal cortex morphology (Pezawas et al., 2004).

The success of these candidate gene studies has led to increased interest in using neuroimaging endophenotypes to study genetic determinants of brain disorders (Hibar et al., 2011a; Thompson et al., 2010). Recently, there has been increased interest in an AD risk gene, *growth factor receptor bound protein 2-associated protein* or *GAB2*. The *GAB2* gene is well characterized as a risk gene for the development of late-onset AD (Chapuis et al., 2008; Lin et al., 2010; Ramirez-Lorca et al., 2009; Reiman et al., 2007). Large meta-analyses confirm that it has a moderate effect on disease risk with an odds ratio of 1.27–1.51, using a 95% confidence interval (Ikram et al., 2009; Schjeide et al., 2009). There is convincing evidence that *GAB2* is expressed throughout the brain and throughout life (Reiman et al., 2007; Trollmann et al., 2010). In our previous study of 731 elderly subjects from the Alzheimer's Disease Neuroimaging Initiative (ADNI), we identified the *GAB2* gene as significantly associated with morphometric brain volume differences using gene-based tests (Hibar et al., 2011b). We showed also that gene-based tests — based on principal component regression (PCReg) encoding the set of single nucleotide polymorphisms (SNPs) in a gene — have more power to detect significant associations than standard univariate statistical methods, in certain cases. The association of *GAB2* with morphometric brain volume differences was undetectable with traditional univariate methods, but showed significant effects in the brain when the cumulative evidence of variation across the gene was incorporated into a gene-based association statistic. Another prior analysis of *GAB2* in a separate, independent dataset found that a protective *GAB2* haplotypic variant is associated with increased glucose metabolism in brain regions typically affected in AD (including the left temporal lobe, right frontal lobe, bilateral parietal lobes, and the precuneus) measured with fluorodeoxyglucose positron emission tomography (FDG-PET) (Liang et al., 2011). In addition, Liang et al. (2011) showed, when studying *APOE*4 allele carriers specifically, that carriers have increased glucose metabolism if they also carry the protective *GAB2* haplotype. Lower levels of glucose metabolism in the brain tissue of AD and mild cognitive impairment (MCI) patients may reflect a decrease in neuronal density, as well as abnormal metabolism (Magistretti & Pellerin, 1996; Mark et al., 1997; Piert et al., 1996). While the Liang et al. (2011) study focused on haplotype blocks, certain gene-based tests, such as PCReg performed by Hibar et al., (2011b), may be considered comparable, as the *GAB2* gene lies in a single linkage-disequilibrium (LD) block (Reiman et al., 2007). This replication of *GAB2* effects in a separate sample and imaging modality lends credibility to *GAB2* as a risk gene that influences the brain. It is then reasonable to suspect that *GAB2* gene variants have significant, observable effects on brain morphology, perhaps even in early adulthood. However, no studies have examined how *GAB2* relates to brain structure in young adults, long before the onset of neurodegeneration. In this study, we hypothesized that gene-based tests in the AD-risk gene, *GAB2*, would reveal significant effects on brain morphology in young adults.

Methods

Subjects

A total of 755 healthy, young adult (mean = 23.1, *SD* = 3.1 years) twins and their siblings (469 females) from 439 families (294 dizygotic twins, 222 monozygotic twins, 143 singletons, three dizygotic trios, and 87 siblings) were examined in this study. All subjects had standard T_1-weighted MRI brain scans and genome-wide genotyping information available. All subjects were of European ancestry and recruited as part of the Queensland Twin Imaging Study (QTIM) in Australia. The QTIM study is an ongoing five-year longitudinal study of healthy young twins with structural and functional MRI, diffusion tensor imaging (DTI), genetics, and comprehensive cognitive assessments (de Zubicaray et al., 2008). Subjects were excluded if they reported any pathologies known to affect the brain, head injuries, or major illnesses. All subjects were right-handed, as determined by the 12-item Annett's handedness questionnaire (Annett, 1970). Informed consent was obtained from each subject and the study was approved by the institutional review boards of the University of California, Los Angeles, and the Queensland Institute of Medical Research.

Genotyping and Quality Control Filtering

Genome-wide genotype data were collected on the Human610-Quad BeadChip (Illumina, Inc., San Diego, CA). Several SNPs were dropped from the dataset based on standard quality control filtering measures used in other large GWAS analyses (Wellcome Trust Case Control Consortium, 2007). Individual SNPs were removed based on the following criteria: call rate < 95% (8,447 SNPs removed), minor allele frequency < .01 (33,347 SNPs removed), significant deviation from Hardy-Weinberg equilibrium $p < 1 \times 10^{-6}$ (2,841 SNPs removed), autosomal chromosomes only, and a platform-specific score of .07 to eliminate blank genotype calls (results in a variable number of missing genotypes for each SNP).

After filtering, the hard genotype calls were imputed to the HapMap Phase II release 21 reference dataset (Altshuler et al., 2010). Imputation was performed using the robust and freely available software, MaCH (Abecasis et al., 2010). The imputed genotypes were further filtered based on minor allele frequency < .01 (38,481 SNPs removed) and R^2 < .3 (54,337 SNPs removed). After imputation, 2,439,807 SNPs passed all quality control criteria.

In this study, we were only interested in SNPs found in the candidate gene, *GAB2*, as it was strongly implicated in our prior study of a different dataset (Hibar et al., 2011b). We used the gene annotation function in the KGG software

package (Li et al., 2011; Li et al., 2010) to select SNPs from our set of imputed genotypes in the *GAB2* gene group. SNPs within 50 Kb upstream or downstream of the *GAB2* gene border were included in the final group of selected SNPs.

Image Acquisition and Processing

High resolution structural MRI scans were obtained for each subject on a single 4-Tesla scanner (Bruker Medspec). T_1-weighted images were acquired with an inversion recovery rapid gradient echo sequence (TI/TR/TE = 700/1500/3.35 ms; flip angle = 8°; slice thickness = 0.9 mm, with a 256^2 acquisition matrix).

Non-brain regions were removed from the T_1-weighted scans using Robex (Iglesias et al., 2011) specifically trained on manually edited skull-stripped images. Next, scans were corrected for image field non-uniformity using FreeSurfer (http://surfer.nmr.mgh.harvard.edu/), and linearly aligned to a common template using a 9-parameter model (Holmes et al., 1998).

3D Maps of Morphometric Brain Differences

The minimum deformation template (MDT) represents a nonlinear average of anatomical differences throughout the brain, and is used as a reference template to help compare the brain structure of subjects in the study. Using the MDT as a target, 3D 'Jacobian' maps of regional brain volume differences were generated for each subject, with a nonlinear, inverse consistent registration algorithm (Leow et al., 2005), and then downsampled to a $2 \times 2 \times 2$ mm isometric voxel size. Each voxel value in the 3D maps measures the difference in volume between the subject's image and the template, based on the gradient of the deformation field required to deform the subject's scan to match the common template. As subjects are all registered to the same MDT, we can examine regional morphometric differences in brain volume by analyzing the determinant of the Jacobian matrix at the same voxel in each subject. In this study, we performed a whole-brain analysis of the volume differences from these 3D morphometric maps for each voxel in the brain and across all subjects.

Gene-Based Tests

Tests of association of the *GAB2* gene with whole-brain, voxel-wise regional brain volume differences were conducted inside the whole-brain mask of the MDT, using PCReg (Wang & Abbott, 2008). PCReg test statistics are generated by first performing principal components analysis (PCA) on a set of *n* SNPs across our sample of subjects. The PCA outputs a set of orthogonal eigenvectors that represent the variance components from the set of SNPs. This transformation is defined so that the first principal component has the largest possible variance (accounts for as much as possible of the variability in the data), and each succeeding component in turn accounts for the highest variance possible under the constraint that it be orthogonal

to (linearly uncorrelated with) the preceding components. Eigenvectors are then selected (in descending order of the amount of variance explained) until they explain at least 95% of the total variance in the original SNP set. These PCA steps provide an efficient means for dimension reduction but, more importantly, they provide a means to test the cumulative evidence for association across a full gene without being vulnerable to problems due to multicollinearity. Association tests with PCReg use a multiple partial-*F* test framework, which works by fitting two separate regression models ('full' and 'reduced') such that the full model contains a set of eigenvectors with age and sex covariates as regressors, and morphometric volume values as the dependent variable. The variance explained by the full model is then compared to the variance explained by a reduced model that fits the age and sex covariates as regressors, with the same morphometric volume values as the dependent variable. An *F* statistic and *p*-value are assigned to each voxel, based on the amount of additional variance explained by the full model compared to the reduced model. Our PCReg tests were implemented using the Efficient Mixed-Model Association (EMMA) software package (Kang et al., 2008). EMMA uses a kinship matrix to control for relatedness in family-based and twin samples, such as this one, using a mixed-effects model.

Multiple Comparisons Correction

Performing a large number of statistical tests at multiple voxels across the brain increases the potential of identifying false-positive findings (i.e., inflating Type I errors). To correct for the total of number of tests performed, and appropriately control Type I errors, we employed the searchlight false discovery rate procedure (searchlight-FDR; Langers et al., 2007). Searchlight-FDR controls for the regional significance of test statistics under the null hypothesis, and incorporates information on the spatial extent of the statistical effects and the smoothness of the underlying image. The searchlight-FDR procedure implemented in this study thresholds statistical maps at the standard $q = .05$ false-positive rate. Correction for the number of 'eigen-SNPs' included in the model is not required, as gene-based tests with PCReg evaluate association with a multiple partial-*F* test that includes the full set of eigen-SNPs in a single statistical test.

Results

The *GAB2* Gene and PCReg

After all quality control filtering, imputation, and annotation, there were 51 SNPs in the *GAB2* gene grouping. Positional and functional annotation data for each SNP in the analysis are shown in Table 1. After applying PCA to the set of 51 SNPs, we found that the first 10 principal components were sufficient to explain 95% of the total variance in

TABLE 1

Gene Annotation Results for the *GAB2* Gene using KGG
Software[a]

SNP	Position	Gene feature	Conservation score
rs10899500	78125246	intron	0.071
rs10899496	78123831	intron	0.009
rs2063724	78133077	-	0.008
rs2511175	77975081	intron	0.075
rs1981405	77976208	intron	0.002
rs948662	77979829	intron	0.202
rs2511170	77980582	intron	0.11
rs10793302	78040961	intron	0.069
rs7115850	78045071	intron	0.001
rs10899488	78088754	intron	0
rs1893447	77973182	intron	0.023
rs2450130	77943457	intron	0.551
rs1017908	77948095	intron	0.128
rs1893448	77969180	intron	0.102
rs2510038	77966034	intron	0.014
rs2510054	77959659	intron	0.005
rs731600	77963133	intron	0.006
rs1007837	77941076	intron	0.001
rs2248407	77937800	coding-synonymous	0.005
rs1385600	77936166	coding-synonymous	0.813
rs1385601	77936064	intron	0.004
rs1318241	77930792	intron	0.063
rs901104	77930499	intron	0.283
rs6592772	78015563	intron	0.008
rs7939646	78111613	intron	0.014
rs4944196	78008731	intron	0.026
rs4945261	77990260	intron	0.005
rs7101429	77992967	intron	0.021
rs10899456	78000155	intron	0.006
rs4291702	78001248	intron	0.001
rs4944195	78003499	intron	0.728
rs11602622	78010830	intron	0.047
rs2450129	77940385	intron	0.459
rs10899469	78018313	intron	0.286
rs4945265	78027458	intron	0.782
rs10899485	78072383	intron	0.003
rs10501426	78057122	intron	0.296
rs2292573	78053139	intron	0.017
rs2292572	78052864	utr-5	0.001
rs2373115	78091150	intron	0.002
rs10899489	78095373	intron	0.016
rs7112234	78102470	intron	0.017
rs1046780	77926769	utr-3	0
rs866901	77926309	near-gene-3	0.003
rs2912	77926292	near-gene-3	0
rs7927923	77979414	intron	0.001
rs3740677	77928036	utr-3	0.025
rs10793294	77996403	intron	0.879
rs11237451	78025459	intron	0.233
rs2450135	77927995	utr-3	0.049
rs11601726	78068039	intron	0.002

Note: SNP = single nucleotide polymorphism. The starting position of
GAB2 (Entrez Gene ID: 9846) on chromosome 11 is 77916336 (base
pairs) with a total length of 222532 (base pairs). For each of the 51
SNPs in our analysis, we give the positional information in base pairs,
annotation of possible SNP function, and a conservation score from
the UCSC Genome Browser (http://hgdownload.cse.ucsc.edu/).
[a] see Li et al. (2011) & Li et al. (2010)

the full SNP set. We used this set of 10 eigen-SNPs in the
PCReg association tests at each voxel across the full brain.

Statistical Parametric Maps

The significant regions of the searchlight-FDR adjusted *p*-
map for the whole-brain *GAB2* association tests is shown
in Figure 1. In total, seven clusters survived the searchlight-
FDR correction (here we use cluster to mean sets of con-
tiguous voxels, even though we used a voxel-wise correction

TABLE 2

A Summary of Clusters Significantly Associated with *GAB2* after
Correction for Multiple Comparisons Using Searchlight FDR

Cluster #	$MNI_{(x)}$	$MNI_{(y)}$	$MNI_{(z)}$	Size (mm^3)	Minimum corrected *p*-value
1	24	−73	42	10696	.0387 (.0019)
2	48	−58	48	2489	.0387 (.0017)
3	−48	−34	20	1884	.0387 (.0016)
4	25	41	44	1164	.0408 (.004)
5	−21	−75	−49	694	.0387 (.0014)
6	67	−24	−3	690	.0387 (.0018)
7	18	−24	−21	117	.0470 (.0045)

Note: MNI = Montreal Neurological Institute. Here we define 'cluster' to
mean any set of significant contiguous voxels after correction for
multiple comparisons. The location of the most highly associated
voxel in each cluster is given in MNI coordinates: $MNI_{(x,y,z)}$. The size
or extent of each cluster is given in mm^3. The minimum corrected
p-value is the most highly associated voxel in a given cluster in the
searchlight-FDR corrected map; uncorrected *p*-values for that voxel
are given in parentheses.

method). The associated regions after correction for multi-
ple comparisons are summarized in Table 2.

Post Hoc Analysis

The multiple partial *F*-test yields *F*-test statistics that are
non-directional (in other words, they do not tell you the
'direction' of an effect). So, for our primary analysis, we
report only *p*-value statistics for each voxel that passes re-
gional FDR correction, using searchlight-FDR. These *p*-
values only indicate that there was a significant association
between *GAB2* and volume differences in the cohort at a
given voxel, not its direction. To get a better idea of the
direction of an effect, we performed a *post hoc* analysis us-
ing the first principal component from the PCA of *GAB2*
SNPs as a regressor, along with age and sex covariates, in a
mixed-effect regression (MER) model (as implemented in
EMMA), at each point across the brain. In this way, we were
able to obtain approximate directional effects of the *GAB2*
gene (i.e., those implied by the first principal component)
on brain volume differences using the *Beta* coefficients from
the MER model (Figure 2).

Discussion

Here we found a significant association between morpho-
logical differences in young-adult brains and variation in
the *GAB2* gene. These results augment our previous work
with the elderly ADNI sample that demonstrated for the
first time that variation in the *GAB2* gene was associated
with observable morphological differences in the brain.
Our study of the QTIM sample expands on the litera-
ture that has established *GAB2* as an AD risk gene. Prior
studies have not considered how this gene might affect the
brain long before the typical age of onset of the disease.
We found significant differences in regional brain volume
in a large region of the right parietal lobe, and additional
smaller significant clusters in the left parietal, and along the
tissue/cerebral spinal fluid (CSF) boundary, in the temporal
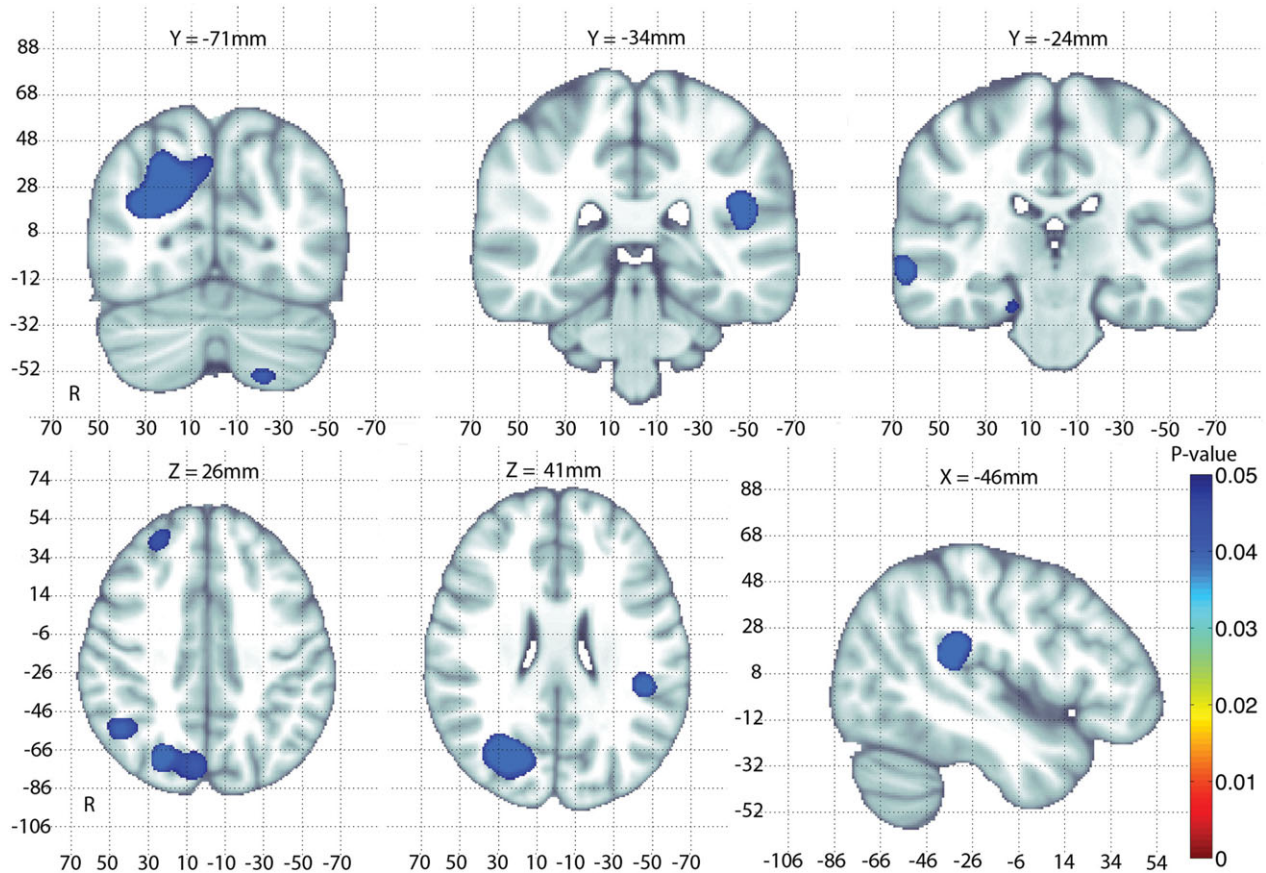
FIGURE 1

An adjusted *p*-map of *GAB2* association tests after correcting for multiple comparisons using searchlight FDR. Adjusted *p*-values < .05 are considered significant and are overlaid on the MNI-152 T1 template for anatomical reference. The largest clusters of significant associations of *GAB2* with morphological differences occur in the right parietal lobe.

lobes of the young-adult twins. A *post hoc* analysis was also performed to determine the direction of the *GAB2* gene effects on brain morphology. There was a negative correlation between overall tissue volume and *GAB2* loading in the right parietal lobe region. In addition, we found a positive correlation between *GAB2* loading and CSF volume along the sulci of the temporal lobes (partial volume effects along the tissue/CSF boundary means that voxels along the border usually represent the effect of CSF volume change), as shown in Figure 2.

Function of *GAB2*

GAB2 encodes a human adapter protein that acts in a number of cell proliferation pathways, especially in endothelial cells (Zhang & Broxmeyer, 2000) and is expressed throughout the human brain (Zhao et al., 1999). The mechanism by which the *GAB2* gene leads to increased neurodegeneration is well understood. Reiman et al. (2007) showed that normally functioning *GAB2* protein is responsible for suppressing the phosphorylation of *tau* tangles associated with the development of Alzheimer's disease. Using small-

interfering RNA (siRNA) to knock-down *GAB2* function, Reiman et al. also demonstrated a significant increase in *tau* tangle formation in neuronal tissue with the *GAB2* protein function diminished. While the role of *GAB2* in the pathway that leads to the formation of *tau* tangles is well understood, there is scant evidence in the literature about functional mechanisms and pathways through which changes in the efficiency of the *GAB2* protein might lead to morphological differences in young-adult brains.

Knowing that an AD risk gene such as *GAB2* may have a detectable effect in the young adult brain is useful, as it may indicate a developmental vulnerability to AD, without directly promoting AD pathology (e.g., amyloid plaque and neurofibrillary tangle formation). This is the most likely scenario as the young-adult brain is fairly low in amyloid deposits (Bartzokis, 2011; Braak & Braak, 1997). Even so, recent studies of some other AD risk genes have also revealed detectable effects in young adults. Shaw et al. (2007) showed that adolescent *APOE*4 allele carriers have a thinner cortex and slower cortical thickening than their *APOE*2/3 counterparts. A genetic variant (rs11136000) in the AD risk gene,
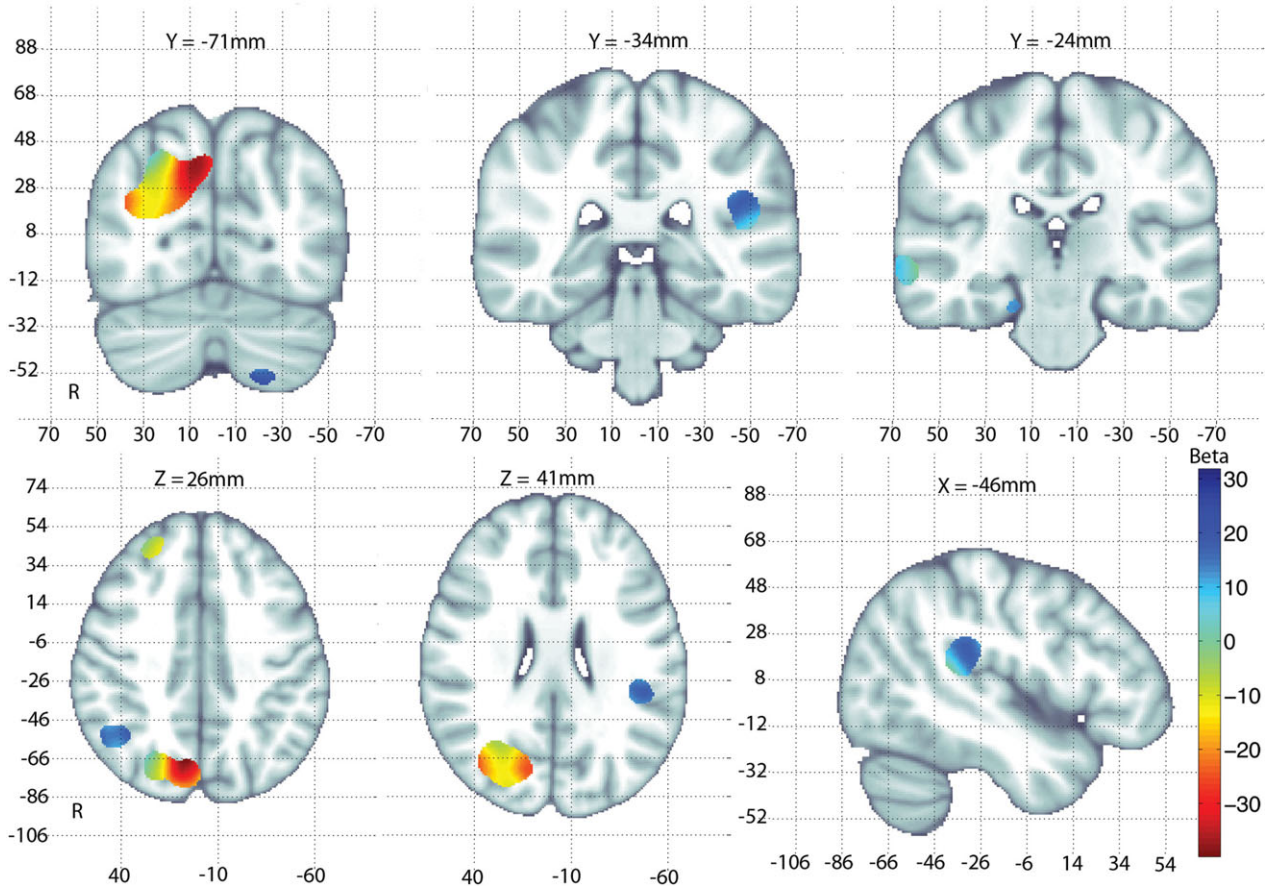
FIGURE 2

Beta coefficient values are shown for the first principal component of the *GAB2* SNPs used in a multiple linear regression with age and sex as covariates. Only regions that were significant after correction for multiple comparisons using searchlight FDR are shown. The coefficient maps are overlaid on the MNI-152 T1 template for anatomical reference. Negative Beta values (warmer colors) in the tissue of the parietal lobe indicate a negative relationship of tissue volume and *GAB2* loading. Positive Beta values (cooler colors) in and around the cerebrospinal fluid of the lateral sulcus and temporal lobes indicate a positive relationship of CSF expansion with *GAB2* loading.

CLU, found in 88% of Caucasian subjects, confers nearly a 20% lifetime increase in the risk for AD and is associated with white matter differences in DTI scans of young adults (Braskie et al., 2011). Similarly, the H63D variant in *HFE*, an iron overload gene, is associated with white matter microstructure in young adults and is thought to be associated with AD risk (Jahanshad et al., 2012).

Conclusions and Interpretations

An essential part of endophenotype theory suggests that complex brain disorders may be better described by traits related to a disease, but with simpler genetic determinants than case-control phenotypes (Gottesman & Gould, 2003). Neuroimaging endophenotypes are now widely used to assess genetic contributions to complex neurodegenerative disorders such as late-onset Alzheimer's disease (LOAD). Given the cost and difficulty of collecting large neuroimaging datasets, it can be challenging to collect enough data for unbiased gene discovery methods such as GWAS (de Geus,

2010). Very large neuroimaging genetics consortia are only just beginning to aggregate samples large enough to discover and replicate GWAS findings from imaging studies (ENIGMA; http://enigma.loni.ucla.edu; Stein et al., 2012). Even so, hypothesis-driven candidate gene studies may be performed in smaller datasets, without such a heavy correction for the number of SNPs assessed. Several such studies of disease risk genes (e.g., *CLU*, Braskie et al., 2011; and *HFE*, Jahanshad et al., 2012) have revealed how variants in these genes affect the brain, offering a plausible mechanistic explanation of how they may promote risk for neurological disease. Endophenotypes can help to localize gene effects, revealing functional and anatomical differences between carriers of different variants; they may also help to classify disease subtypes that may not be apparent in case-control studies (de Geus, 2010).

The current study shows detectable associations between the AD risk gene *GAB2* and morphological brain differences in young adults. Our findings build on our previous work

in a separate cohort of elderly subjects that shows significant morphological differences associated with variation in the *GAB2* gene (Hibar et al., 2011b). While we report significant associations in the right parietal lobe, lateral sulcus, and bilateral temporal lobes, none of the voxels overlap with the voxels that survived statistical thresholding in the original ADNI sample. In this analysis, we performed an unbiased search across each voxel of the full brain without incorporating information from our prior tests in the ADNI dataset. The reason for this is that voxels that are significant after correction for multiple comparisons do not necessarily represent the only voxels where *GAB2* may have an effect. We wanted to perform an analysis that allowed for the possibility to observe an effect anywhere in the brain. As such, the most appropriate test is a brain-wide search, as it asserts only that the gene has some effect in the brain, rather than making a stronger assertion about its specific localization. In addition, the QTIM dataset differs substantially from the ADNI dataset (subjects are, on average, around 50 years younger in the QTIM study, and are scanned at a different field strength on a different continent). Given this, the regions where *GAB2* is associated with brain morphology may be very different from those observed in the elderly ADNI sample. From a biological point of view, it may also be that a gene has regional effects on the brain that either spread out or become more regionally specific over the human lifespan. Or, perhaps more likely, it could be that a very weak effect is spread over the entire brain in both samples, but due to noise and anatomical variability in the two cohorts, different locations in the brain contribute to the statistical results in each cohort. As an alternative, more stringent, approach, a conjunction test (Nichols et al., 2005) could be performed to directly identify voxels where a gene effect is statistically significant in several cohorts at once. Such tests have relatively low power, as they require that the gene effect be found consistently in the same voxels in all cohorts, rather than across the brain in aggregate in each cohort. Different formulations of the null hypothesis may therefore greatly affect the power and scope of the inferences. We found a large set of significant voxels in the parietal and temporal lobes that were associated with tissue volume differences. Regions of both the parietal and temporal lobes have been associated with susceptibility for and progression of Alzheimer's disease (Leow et al., 2009). Parietal lobe atrophy (Scahill et al., 2002), impaired white matter microstructure (Bozzali et al., 2002), and glucose hypometabolism (Langbaum et al., 2009), are well-studied effects of Alzheimer's disease progression on the brain. Additionally, Liang et al. (2011) showed reduced glucose metabolism bilaterally in the parietal and temporal lobes of carriers of a *GAB2* haplotypic risk variant. Many of the significant regions from that study appear to overlap with the regions found in this study, especially in the parietal lobes. Volume changes in the temporal lobes, specifically, have been commonly used as a biomarker for tracking the progression of Alzheimer's disease, and also for image-based diagnostic classification (Jack et al., 1998; Jack et al., 1997). Here we found that *GAB2* is associated with differences in regional brain volumes in young adults, in regions strongly implicated in the progression of Alzheimer's disease. This adds support to the notion that *GAB2* may be used to help identify individuals at heightened risk for AD long before the onset of disease.

Further replication of observed effects of the *GAB2* gene in young adults is still required in order to aggregate evidence about true morphological effects. While searching for genetic determinants of morphological brain differences, the interpretation of results should consider not only individual genetic contributions, but potentially correlated alleles as well. In our study, we detected a very mild positive correlation of the 51 SNPs from the *GAB2* gene and the *CLU* Alzheimer's disease risk SNP rs11136000 (Pearson's $r = .07–.08$), though none of the test statistics passed a Bonferroni correction for the number of SNPs tested ($p < 9.8 \times 10^{-4}$). Tests of other major candidate gene SNPs, such as the *BDNF* Val66Met polymorphism (Chiang et al., 2010), and the H63D polymorphism of the *HFE* gene (Jahanshad et al., 2012), showed no evidence of positive correlation. There could, in principle, be correlations between risk alleles, especially in an elderly population, due to a survivor effect. This could arise if adverse variants in a gene were associated with early mortality. Protective variants might then be present together in the survivors more frequently than their random co-occurrence in randomly selected people. Our analysis provides new evidence for an association between morphological differences and variation in the *GAB2* in young adults, long before the onset of AD pathology. We hope that our findings will inform future research on the functional relevance of *GAB2* in neural development.

Acknowledgments

References

Abecasis, G. R., Li, Y., Willer, C. J., Ding, J., & Scheet, P. (2010). MaCH: Using sequence and genotype data to estimate haplotypes and unobserved genotypes. *Genetic Epidemiology, 34*, 816–834.

Akil, H., Brenner, S., Kandel, E., Kendler, K. S., King, M. C., Scolnick, E., Watson, J. D., & Zoghbi, H. Y. (2010). Medicine. The future of psychiatric research: Genomes and neural circuits. *Science, 327*, 1580–1581.

Altshuler, D. M., Gibbs, R. A., Peltonen, L., Dermitzakis, E., Schaffner, S. F., Yu, F., et al. (2010). Integrating common and rare genetic variation in diverse human populations. *Nature, 467*, 52–58.

Annett, M. (1970). A classification of hand preference by association analysis. *British Journal of Psychology, 61*, 303–321.

Bartzokis, G. (2011). Alzheimer's disease as homeostatic responses to age-related myelin breakdown. *Neurobiology of Aging, 32*, 1341–1371.

Bis, J. C., DeCarli, C. S., Smith, A. V., van der Lijn, F., Crivello, F., Fornage, M., . . . Seshadri, S., for the Cohorts for Heart and Aging Research in Genomic Epidemiology (CHARGE) Consortium. (2012). Common variants at 12q14 and 12q24 are associated with hippocampal volume. *Nature Genetics*, *44*, 545–551.

Bozzali, M., Falini, A., Franceschi, M., Cercignani, M., Zuffi, M., Scotti, G., Comi, G., & Filippi, M. (2002). White matter damage in Alzheimer's disease assessed in vivo using diffusion tensor magnetic resonance imaging. *Journal of Neurology, Neurosurgery, and Psychiatry, 72*, 742–746.

Braak, H., & Braak, E. (1997). Frequency of stages of Alzheimer-related lesions in different age categories. *Neurobiology of Aging, 18*, 351–357.

Braskie, M. N., Jahanshad, N., Stein, J. L., Barysheva, M., McMahon, K. L., de Zubicaray, G. I., Martin, N. G., Wright, M. J., Ringman, J. M., Toga, A. W., & Thompson, P. M. (2011). Common Alzheimer's disease risk variant within the *CLU* gene affects white matter microstructure in young adults. *Journal of Neuroscience, 31*, 6764–6770.

Chapuis, J., Hannequin, D., Pasquier, F., Bentham, P., Brice, A., Leber, I., Frebourg, T., Deleuze, J. F., Cousin, E., Thaker, U., Amouyel, P., Mann, D., Lendon, C., Campion, D., & Lambert, J. C. (2008). Association study of the *GAB2* gene with the risk of developing Alzheimer's disease. *Neurobiology of Disease, 30*, 103–106.

Chiang, M. C., Barysheva, M., Toga, A. W., Medland, S. E., Hansell, N. K., James, M. R., McMahon, K. L., de Zubicaray, G. I., Martin, N. G., Wright, M. J., & Thompson, P. M. (2010). *BDNF* gene effects on brain circuitry replicated in 455 twins. *Neuroimage, 15*, 448–454.

de Geus, E. J. (2010). From genotype to EEG endophenotype: A route for post-genomic understanding of complex psychiatric disease? *Genome Medicine, 2*, 63.

de Zubicaray, G. I., Chiang, M. C., McMahon, K. L., Shattuck, D. W., Toga, A. W., Martin, N. G., Wright, M. J., & Thompson, P. M. (2008). Meeting the challenges of neuroimaging genetics. *Brain Imaging and Behavior, 2*, 258–263.

Fernandes, B. S., Gama, C. S., Cereser, K. M., Yatham, L. N., Fries, G. R., Colpo, G., de Lucena, D., Kunz, M., Gomes, F. A., & Kapczinski, F. (2011). Brain-derived neurotrophic factor as a state-marker of mood episodes in bipolar disorders: A systematic review and meta-regression analysis. *Journal of Psychiatric Research, 45*, 995–1004.

Gogtay, N., Hua, X., Stidd, R., Boyle, C. P., Lee, S., Weisinger, B., Chavez, A., Giedd, J. N., Clasen, L., Toga, A. W., Rapoport, J. L., & Thompson, P. M. (in press). Delayed white matter growth trajectory in young non-psychotic siblings of childhood-onset schizophrenia patients. *Archives of General Psychiatry*.

Gottesman, I. I., & Gould, T. D. (2003). The endophenotype concept in psychiatry: Etymology and strategic intentions. *The American Journal of Psychiatry, 160*, 636–645.

Green, M. J., Matheson, S. L., Shepherd, A., Weickert, C. S., & Carr, V. J. (2011). Brain-derived neurotrophic factor levels in schizophrenia: A systematic review with meta-analysis. *Molecular Psychiatry, 16*, 960–972.

Hajek, T., Kopecek, M., & Hoschl, C. (2012). Reduced hippocampal volumes in healthy carriers of brain-derived neurotrophic factor Val66Met polymorphism: Meta-analysis. *World Journal of Biological Psychiatry, 13*, 178–187.

Hibar, D. P., Kohannim, O., Stein, J. L., Chiang, M.-C., & Thompson, P. M. (2011a). Multilocus genetic analysis of brain images. [Review]. *Frontiers in Genetics, 2*, 73.

Hibar, D. P., Stein, J. L., Kohannim, O., Jahanshad, N., Saykin, A. J., Shen, L., Kim, S., Pankratz, N., Foroud, T., Huentelman, M. J., Potkin, S. G., Jack, C. R. Jr., Weiner, M. W., Toga, A. W., Thompson, P. M., & Alzheimer's Disease Neuroimaging Initiative. (2011b). Voxelwise gene-wide association study (vGeneWAS): Multivariate gene-based association testing in 731 elderly subjects. *NeuroImage, 56*, 1875–1891.

Holmes, C. J., Hoge, R., Collins, L., Woods, R., Toga, A. W., & Evans, A. C. (1998). Enhancement of MR images using registration for signal averaging. *Journal of Computer Assisted Tomography, 22*, 324–333.

Iglesias, J. E., Liu, C. Y., Thompson, P. M., & Tu, Z. (2011). Robust brain extraction across datasets and comparison with publicly available methods. *IEEE Transactions on Medical Imaging, 30*, 1617–1634.

Ikram, M. A., Liu, F., Oostra, B. A., Hofman, A., van Duijn, C. M., & Breteler, M. M. B. (2009). The *GAB2* Gene and the Risk of Alzheimer's Disease: Replication and Meta-Analysis. *Biological Psychiatry, 65*, 995–999.

Jack, C. R., Petersen, R. C., Xu, Y., O'Brien, P. C., Smith, G. E., Ivnik, R. J., Tangalos, E. G., & Kokmen, E. (1998). Rate of medial temporal lobe atrophy in typical aging and Alzheimer's disease. *Neurology, 51*, 993–999.

Jack, C. R., Petersen, R. C., Xu, Y. C., Waring, S. C., O'Brien, P. C., Tangalos, E. G., Smith, G. E., Ivnik, R. J., & Kokmen, E. (1997). Medial temporal atrophy on MRI in normal aging and very mild Alzheimer's disease. *Neurology, 49*, 786–794.

Jahanshad, N., Kohannim, O., Hibar, D. P., Stein, J. L., McMahon, K. L., de Zubicaray, G. I., Medland, S. E., Montgomery, G. W., Whitfield, J. B., Martin, N. G., Wright, M. J., Toga, A. W., & Thompson, P. M. (2012). Brain structure in healthy adults is related to serum transferrin and the H63D polymorphism in the *HFE* gene. *Proceedings of the National Academy of Sciences USA, 109*, E851–859.

Kang, H. M., Zaitlen, N. A., Wade, C. M., Kirby, A., Heckerman, D., Daly, M. J., & Eskin, E. (2008). Efficient control of population structure in model organism association mapping. *Genetics, 178*, 1709–1723.

Kremen, W. S., Prom-Wormley, E., Panizzon, M. S., Eyler, L. T., Fischl, B., Neale, M. C., Franz, C. E., Lyons, M. J., Pacheco, J., Perry, M. E., Stevens, A., Schmitt, J. E., Grant, M. D., Seidman, L. J., Thermenos, H. W., Tsuang, M. T., Eisen, S. A., Dale, A. M., & Fennema-Notestine, C. (2010). Genetic and environmental influences on the size of specific brain regions in midlife: The VETSA MRI study. *NeuroImage, 49*, 1213–1223.

Langbaum, J. B. S., Chen, K., Lee, W., Reschke, C., Bandy, D., Fleisher, A. S., Alexander, G. E., Foster, N. L., Weiner, M. W., Koeppe, R. A., Jagust, W. J., Reiman, E. M., & Alzheimer's Disease Neuroimaging Initiative. (2009). Categorical and correlational analyses of baseline fluorodeoxyglucose positron emission tomography images from the Alzheimer's Disease Neuroimaging Initiative (ADNI). *NeuroImage, 45*, 1107–1116.

Langers, D. R., Jansen, J. F., & Backes, W. H. (2007). Enhanced signal detection in neuroimaging by means of regional control of the global false discovery rate. *NeuroImage, 38*, 43–56.

Leow, A., Huang, S. C., Geng, A., Becker, J., Davis, S., Toga, A., & Thompson, P. (2005). Inverse consistent mapping in 3D deformable image registration: its construction and statistical properties. *Information Processing in Medical Imaging, 19*, 493–503.

Leow, A. D., Yanovsky, I., Parikshak, N., Hua, X., Lee, S., Toga, A. W., Jack, C. R., Bernstein, M. A., Britson, P. J., Gunter, J. L., Ward, C. P., Borowski, B., Shaw, L. M., Trojanowski, J. Q., Fleisher, A. S., Harvey, D., Kornak, J., Schuff, N., Alexander, G. E., Weiner, M. W., Thompson, P. M., & Alzheimer's Disease Neuroimaging Initiative. (2009). Alzheimer's Disease Neuroimaging Initiative: A one-year follow up study using tensor-based morphometry correlating degenerative rates, biomarkers and cognition. *NeuroImage, 45*, 645–655.

Li, M. X., Gui, H. S., Kwan, J. S. H., & Sham, P. C. (2011). GATES: A rapid and powerful Gene-Based Association Test using Extended Simes procedure. *American Journal of Human Genetics, 88*, 283–293.

Li, M. X., Sham, P. C., Cherny, S. S., & Song, Y. Q. (2010). A knowledge-based weighting framework to boost the power of genome-wide association studies. *PLoS One, 5*, e14480.

Liang, W. S., Chen, K. W., Lee, W., Sidhar, K., Corneveaux, J. J., Allen, A. N., Myers, A., Villa, S., Meechoovet, B., Pruzin, J., Bandy, D., Fleisher, A. S., Langbaum, J. B., Huentelman, M. J., Jensen, K., Dunckley, T., Caselli, R. J., Kaib, S., & Reiman, E. M. (2011). Association between *GAB2* haplotype and higher glucose metabolism in Alzheimer's disease-affected brain regions in cognitively normal *APOE* epsilon 4 carriers. *NeuroImage, 58*, 974–974.

Lin, K., Tang, M., Han, H., Guo, Y., Lin, Y., & Ma, C. (2010). *GAB2* is not associated with late-onset Alzheimer's disease in Chinese Han. *Neurological Science, 31*, 277–281.

Magistretti, P. J., & Pellerin, L. (1996). Cellular bases of brain energy metabolism and their relevance to functional brain imaging: Evidence for a prominent role of astrocytes. *Cerebral Cortex, 6*, 50–61.

Mark, R. J., Pang, Z., Geddes, J. W., Uchida, K., & Mattson, M. P. (1997). Amyloid beta-peptide impairs glucose transport in hippocampal and cortical neurons: Involvement of membrane lipid peroxidation. *The Journal of Neuroscience, 17*, 1046–1054.

Meyer-Lindenberg, A., & Weinberger, D. R. (2006). Intermediate phenotypes and genetic mechanisms of psychiatric disorders. *Nature Reviews Neuroscience, 7*, 818–827.

Nichols, T., Brett, M., Andersson, J., Wager, T., & Poline, J.-B. (2005). Valid conjunction inference with the minimum statistic. *NeuroImage, 25*, 653–660.

Peper, J. S., Brouwer, R. M., Boomsma, D. I., Kahn, R. S., & Hulshoff Pol, H. E. (2007). Genetic influences on human brain structure: A review of brain imaging studies in twins. *Human Brain Mapping, 28*, 464–473.

Pezawas, L., Verchinski, B. A., Mattay, V. S., Callicott, J. H., Kolachana, B. S., Straub, R. E., Egan, M. F., Meyer-Lindenberg, A., & Weinberger, D. R. (2004). The brain-derived neurotrophic factor val66met polymorphism and variation in human cortical morphology. *Journal of Neuroscience, 24*, 10099–10102.

Piert, M., Koeppe, R. A., Giordani, B., Berent, S., & Kuhl, D. E. (1996). Diminished glucose transport and phosphorylation in Alzheimer's disease determined by dynamic FDG-PET. *Journal of Nuclear Medicine, 37*, 201–208.

Ramirez-Lorca, R., Boada, M., Saez, M. E., Hernandez, I., Mauleon, A., Rosende-Roca, M., Martinez-Lage, P., Gutierrez, M., Real, L. M., Lopez-Arrieta, J., Gayan, J., Antunez, C., Gonzalez-Perez, A., Tarraga, L., & Ruiz, A. (2009). *GAB2* gene does not modify the risk of Alzheimer's disease in Spanish *APOE* 4 carriers. *Journal of Nutrition Health and Aging, 13*, 214–219.

Reiman, E. M., Webster, J. A., Myers, A. J., Hardy, J., Dunckley, T., Zismann, V. L., Joshipura, K. D., Pearson, J. V., Hu-Lince, D., Huentelman, M. J., Craig, D. W., Coon, K. D., Liang, W. S., Herbert, R. H., Beach, T., Rohrer, K. C., Zhao, A. S., Leung, D., Bryden, L., Marlowe, L., Kaleem, M., Mastroeni, D., Grover, A., Heward, C. B., Ravid, R., Rogers, J., Hutton, M. L., Melquist, S., Petersen, R. C., Alexander, G. E., Caselli, R. J., Kukull, W., Papassotiropoulos, A., & Stephan, D. A. (2007). *GAB2* alleles modify Alzheimer's risk in *APOE* epsilon4 carriers. *Neuron, 54*, 713–720.

Scahill, R. I., Schott, J. M., Stevens, J. M., Rossor, M. N., & Fox, N. C. (2002). Mapping the evolution of regional atrophy in Alzheimer's disease: Unbiased analysis of fluid-registered serial MRI. *Proceedings of the National Academy of Sciences of the United States of America, 99*, 4703–4707.

Schjeide, B. M., Hooli, B., Parkinson, M., Hogan, M. F., DiVito, J., Mullin, K., Blacker, D., Tanzi, R. E., & Bertram, L. (2009). *GAB2* as an Alzheimer disease susceptibility gene: Follow-up of genome-wide association results. *Archives of Neurology, 66*, 250–254.

Shaw, P., Lerch, J. P., Pruessner, J. C., Taylor, K. N., Rose, A. B., Greenstein, D., Clasen, L., Evans, A., Rapoport, J. L., & Giedd, J. N. (2007). Cortical morphology in children and adolescents with different apolipoprotein E gene polymorphisms: An observational study. *Lancet Neurology, 6*, 494–500.

Stein, J. L., Medland, S. E., Arias Vasquez, A., Hibar, D. P., Senstad, R. E., Winkler, A. M., . . . Thompson, P. M., for the Enhancing Neuro Imaging Genetics through Meta-Analysis (ENIGMA) Consortium. (2012). Identification of common variants associated with human hippocampal and intracranial volumes. *Nature Genetics, 44*, 552–561.

Thompson, P. M., Cannon, T. D., Narr, K. L., van Erp, T., Poutanen, V. P., Huttunen, M., Lönnqvist, J., Standertskjöld-Nordenstam, C. G., Kaprio, J., Khaledy, M., Dail, R., Zoumalan, C. I., & Toga, A. W. (2001). Genetic influences on brain structure. *Nature Neuroscience, 4*, 1253–1258.

Thompson, P. M., Martin, N. G., & Wright, M. J. (2010). Imaging genomics. *Current Opinion in Neurology, 23*, 368–373.

Trollmann, R., Rehrauer, H., Schneider, C., Krischke, G., Huemmler, N., Keller, S., Rascher, W., & Gassmann, M. (2010). Late-gestational systemic hypoxia leads to a similar early gene response in mouse placenta and developing brain. *American Journal of Physiology: Regulatory, Integrative and Comparative Physiology, 299*, R1489–1499.

Wang, K., & Abbott, D. (2008). A principal components regression approach to multilocus genetic association studies. *Genetic Epidemiology, 32*, 108–118.

Wellcome Trust Case Control Consortium. (2007). Genome-wide association study of 14,000 cases of seven common diseases and 3,000 shared controls. *Nature, 447*, 661–678.

Zhang, S., & Broxmeyer, H. E. (2000). Flt3 ligand induces tyrosine phosphorylation of *gab1* and *gab2* and their association with *shp-2*, grb2, and PI3 kinase. *Biochemical and Biophysical Research Communications, 277*, 195–199.

Zhao, C., Yu, D. H., Shen, R., & Feng, G. S. (1999). *GAB2*, a new pleckstrin homology domain-containing adapter protein, acts to uncouple signaling from ERK kinase to Elk-1. *The Journal of Biological Chemistry, 274*, 19649–19654.